B850 Ring from Photosynthetic Complex LH2 – Comparison of Different Static Disorder Types

Pavel Heřman, David Zapletal

Abstract— Properties of light–harvesting (LH) pigment–protein complexes are strongly influenced by their interactions with environment. These interactions could be modeled by static and dynamic disorder. Influence of static disorder on B850 ring from LH2 complex of purple bacteria is investigated in present paper. The nearest neighbour approximation model of the ring is considered. Four types of uncorrelated Gaussian static disorder (fluctuations of transfer integrals, fluctuations of radial positions of molecules on the ring, fluctuations of angular positions of molecules on the ring and fluctuations of directions of molecular dipole moments) are taking into account. The most important statistical properties of the nearest neighbour transfer integral distributions for different strengths of static disorder are calculated. Results obtained for four above mentioned types of static disorder are discussed and compared.

Keywords—LH2 complex, B850 ring, static disorder, Hamiltonian, transfer integral distributions

I. INTRODUCTION

PHOTOSYNTHESIS is the process by which green plants and certain other organisms (bacteria, blue–green algae) transform light energy into chemical energy. During this process light energy is captured and used to convert water, carbon dioxide, and minerals into oxygen and energy–rich organic compounds. In chemical terms, photosynthesis is a light–energized oxidation–reduction process. Oxidation refers to the removal of electrons from a molecule; reduction refers to the gain of electrons by a molecule. These reactions occur in two stages: the light stage, consisting of photochemical (i.e., light–capturing) reactions; and the dark stage, comprising chemical reactions controlled by enzymes. During the first stage, the energy of light is absorbed and used to drive a series of electron transfers, resulting in the synthesis of ATP and the electron–donor reduced nicotine adenine dinucleotide phosphate (NADPH). During the dark stage, the ATP and NADPH formed in the light–capturing reactions are used to reduce carbon dioxide to organic carbon compounds [1].

Our interest is mainly focused on first (light) stage of photosynthesis in purple bacteria. Solar photons are absorbed by a complex system of membrane–associated pigment–proteins (light–harvesting (LH) antenna) and the electronic excited state is efficiently transferred to a reaction center, where the light energy is converted into a chemical energy [2]. The antenna systems of photosynthetic units from purple bacteria are formed by ring units LH1, LH2, LH3, and LH4. The geometric structure is known in great detail from X–ray crystallography. The general organization of above mentioned light–harvesting complexes is the same: identical subunits are repeated cyclically in such a way that a ring–shaped structure is formed. However the symmetries of these rings are different.

Crystal structure of LH2 complex contained in purple bacterium *Rhodopseudomonas acidophila* was first described in high resolution by McDermott et al. [3], then further e.g. by Papiz et al. [4]. The bacteriochlorophyll (BChl) molecules are organized in two concentric rings. One ring (B800 ring) features a group of nine well–separated BChl molecules with absorption band at about 800 nm. The second ring (B850 ring) consists of eighteen closely packed BChl molecules (B850) absorbing around 850 nm. Dipole moments in LH2 ring have tangential arrangement. The whole LH2 complex is nonameric, it consists of nine identical subunits. LH2 complexes from other purple bacteria have analogous ring structure.

Some bacteria contain also other types of complexes such as the B800–820 LH3 complex (*Rhodopseudomonas acidophila* strain 7050) or LH4 complex (*Rhodopseudomonas palustris*). LH3 complex like LH2 one is usually nonameric but LH4 one is octameric (it consists of eight identical subunits). They can also differ in orientation of molecular dipole moments and strength of mutual interactions between bacteriochorophylls. For instance, interactions between the nearest neighbour bacteriochlorophylls in B–α/B–β ring from LH4 complex are approximately two times smaller in comparison with B850 ring from LH2 complex and they have opposite sign.

The intermolecular distances under 1 nm determine

strong exciton couplings between corresponding pigments. That is why an extended Frenkel exciton states model could be used in theoretical approach. In spite of extensive investigation, the role of the protein moiety in governing the dynamics of the excited states has not been totally clear yet. At room temperature the solvent and protein environment fluctuates with characteristic time scales ranging from femtoseconds to nanoseconds. The simplest approach is to substitute fast fluctuations by dynamic disorder and slow fluctuations by static disorder.

Static disorder effect on the anisotropy of fluorescence for LH2 complexes was studied by Kumble and Hochstrasser [6] and Nagarajan et al. [7], [8]. We extended these investigations by consideration of dynamic disorder. We studied this effect for simple model systems [9]–[11] and then for models of B850 ring (from LH2) [12], [13]. Various types of uncorrelated static disorder (in local excitation energies, in transfer integrals, etc.) and correlated one (e.g., elliptical deformation) were used in the past [14]–[16] and also different arrangements of optical dipole moments were compared [17]–[20]. Recently we have focused on the modelling of absorption and steady state fluorescence spectra of LH2 and LH4 complexes within the nearest neighbour approximation model [21]–[25]. We have also extended our model to full Hamiltonian model and published the results for different types of static disorder [26]–[34].

Main goal of the present paper is the investigation of four types of static disorder (Gaussian fluctuations in transfer integrals, in radial positions of molecules on the ring, in angular positions of molecules on the ring and in directions of dipole moments of molecules) and comparison of their influence on Hamiltonian of B850 ring from LH2 complex. The rest of the paper is structured as follows. Section II introduces the ring model with different types of static disorder, used units and parameters could be found in Section III, results are presented and discussed in Section IV and some conclusions are drawn in Section V.

II. MODEL

We consider only one exciton on molecular ring which can model B850 ring from LH2 complex. The Hamiltonian of an exciton on this ring reads

$$H = H_{\text{ex}}^0 + H_{\text{ph}} + H_{\text{ex}-\text{ph}} + H_{\text{s}}. \qquad (1)$$

A. Ideal ring

First term in Eq. (1),

$$H_{\text{ex}}^0 = \sum_{m=1}^{N} E_m^0 a_m^\dagger a_m + \sum_{m,n=1(m \neq n)}^{N} J_{mn}^0 a_m^\dagger a_n, \qquad (2)$$

corresponds to an exciton, e.g. the system without any disorder. The operator $a_m^\dagger$ (a_m) creates (annihilates) an

exciton at site m, E_m^0 is the local excitation energy of m–th molecule and J_{mn}^0 (for $m \neq n$) is the so–called transfer integral between sites m and n. Local excitation energies E_m^0 are the same for all bacteriochlorophylls on unperturbed ring, i.e.

$$E_m^0 = E_0, \quad m = 1, \ldots, N.$$

Inside one ring the pure exciton Hamiltonian H_{ex}^0 can be diagonalized using the wave vector representation with corresponding delocalized Bloch states α and energies E_α. Using Fourier transformed excitonic operators a_α, the Hamiltonian in α–representation reads

$$H_{\text{ex}}^0 = \sum_{\alpha=1}^{N} E_\alpha a_\alpha^\dagger a_\alpha. \qquad (3)$$

The interaction strengths between the nearest neighbour bacteriochlorophylls inside one subunit and between subunits are almost the same in B850 ring from LH2 complex (see Figure 1 (B) in [5]). That is why such ring can be modeled as homogeneous case. If we consider the nearest neighbour approximation model (only the nearest neighbour transfer matrix elements are nonzero), we have

$$J_{mn}^0 = J_0(\delta_{m,n+1} + \delta_{m,n-1}). \qquad (4)$$

In that case the form of operators a_α is

$$a_\alpha = \sum_{n=1}^{N} a_n e^{i\alpha n}, \ \alpha = \frac{2\pi}{N}l, \ l = 0, \ldots, \pm\frac{N}{2}, \quad (5)$$

where $N = 18$ and the simplest exciton Hamiltonian for B850 ring from LH2 complex in α–representation is given by Eq. (3) with

$$E_\alpha = E_0 - 2J_0 \cos \alpha. \qquad (6)$$

In dipole–dipole approximation, transfer integrals J_{mn} can be written as

$$J_{mn} = \frac{\vec{d}_m \cdot \vec{d}_m}{|\vec{r}_{mn}|^3} - 3\frac{\left(\vec{d}_m \cdot \vec{r}_{mn}\right)\left(\vec{d}_n \cdot \vec{r}_{mn}\right)}{|\vec{r}_{mn}|^5} =$$
$$= |\vec{d}_m||\vec{d}_n|\frac{\cos \varphi_{mn} - 3\cos \varphi_m \cos \varphi_n}{|\vec{r}_{mn}|^3}. \qquad (7)$$

Here $\vec{d}_m$ and $\vec{d}_n$ are local dipole moments of m–th and n–th molecule respectively, $\vec{r}_{mn}$ is the vector connecting m–th and n–th molecule and φ_m (φ_n) is the angle between $\vec{d}_m$ ($\vec{d}_n$) and $\vec{r}_{mn}$. The angle between m–th and n–th vector of local dipole moment ($\vec{d}_m$, $\vec{d}_n$) is referred to as φ_{mn}. Geometric arrangement of the ring has to correspond with the interaction strengths between the nearest neighbour bacteriochlorophylls. That is why distances $r_{m,m+1}$ of neighbouring molecules in B850 ring from the LH2 complex have to be the same (without any disorder) and angles $\beta_{m,m+1}$ have to be the same too ($\beta_{m,m+1} = 2\pi/18$, see Figure 1).
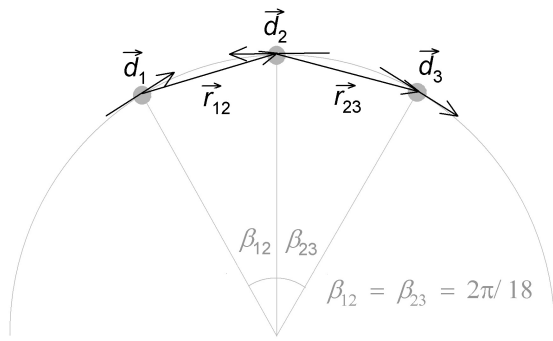
Fig. 1. Geometric arrangement of ideal B850 ring from LH2 complex (without any fluctuations)

B. Dynamic disorder

The second term in Eq. (1),

$$H_{\text{ph}} = \sum_q \hbar \omega_q b_q^\dagger b_q, \tag{8}$$

represents phonon bath in harmonic approximation. Phonon creation and annihilation operators are denoted by $b_q^\dagger$ and b_q, respectively.

The third term,

$$H_{\text{ex-ph}} = \frac{1}{\sqrt{N}} \sum_m \sum_q G_q^m \hbar \omega_q a_m^\dagger a_m (b_q^\dagger + b_q), \tag{9}$$

describes exciton–phonon interaction which is assumed to be site–diagonal and linear in bath coordinates (the term G_q^m denotes the exciton–phonon coupling constant).

C. Static disorder

Last term in Eq. (1), H_s, corresponds to static disorder. Different types of static disorder can be taken into account. Fluctuations in local excitation energies of bacteriochlorophylls $\delta \varepsilon_m$,

$$E_m = E_0 + \delta \varepsilon_m, \tag{10}$$

represent one of the most commonly used types of static disorder.

Consideration of fluctuations in transfer integrals δJ_{mn} ($m \neq n$),

$$J_{mn} = J_{nm} = J_{mn}^0 + \delta J_{mn}, \tag{11}$$

is another way how the static disorder can be modeled. δJ_{mn} can be treated as uncorrelated Gaussian fluctuations (with the standard deviation Δ_J) or they can be connected with deviation in geometric arrangement of the ring. In following, from various types of geometric deviations we deal with three ones:

a) uncorrelated fluctuations of radial positions of molecules δr_m on the ring (Gaussian distribution and standard deviation Δ_r),

$$r_m = r_0 + \delta r_m, \tag{12}$$

where r_0 is the radius of the ring without any disorder (see Figure 2);
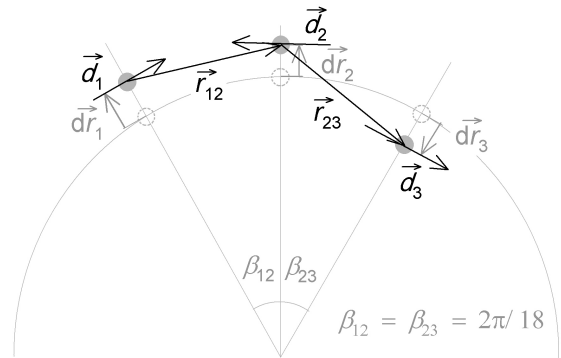

Fig. 2. B850 ring from LH2 complex – fluctuations in radial positions of bacteriochlorophylls δr_m

b) uncorrelated fluctuations of angular positions of molecules $\delta \nu_m$ on the ring (Gaussian distribution and standard deviation Δ_ν),

$$\nu_m = \nu_m^0 + \delta \nu_m, \tag{13}$$

where ν_m^0 is the angular position of m–th batheriochorophyll on the ring, directions of bacteriochlorophyll dipole moments in new positions are again tangential to the ring (see Figure 3);
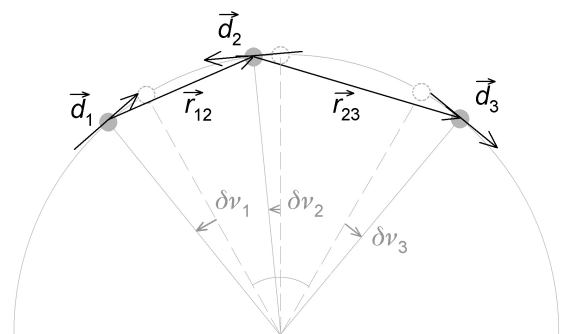

Fig. 3. B850 ring from LH2 complex – fluctuations in angular positions of bacteriochlorophylls $\delta \nu_m$

c) uncorrelated fluctuations of bacteriochlorophyll dipole moment directions $\delta \vartheta_m$ (Gaussian distribution and standard deviation Δ_ϑ)

$$\vartheta_m = \vartheta_m^0 + \delta \vartheta_m, \tag{14}$$

where ϑ_m^0 determines dipole moment direction of m–th bacteriochlorophyll molecule. Positions of bacteriochlorophylls remain the same as in unperturbed ring (see Figure 4).

Only fluctuations in ring plane are considered for all three above mentioned types of static disorder connected with ring geometry.
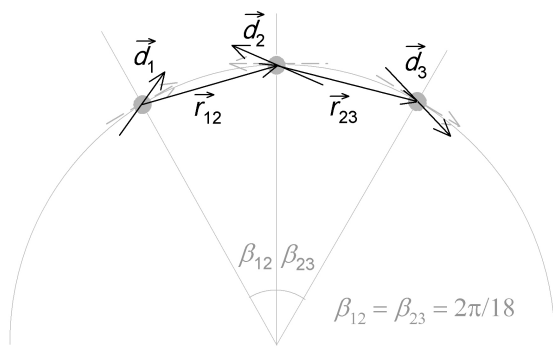
Fig. 4. B850 ring from LH2 complex – fluctuations in directions of bacteriochlorophyll dipole moments $\delta\vartheta_m$

III. Units and Parameters

Dimensionless energies normalized to the transfer integral $J_{m,m+1} = J_0$ (see Eq. (4)) have been used in our calculations. Estimation of J_0 varies in literature between 250 cm^{-1} and 400 cm^{-1}.

In our previous investigations [35] we found from comparison with experimental results for B850 ring from the LH2 complex [36] that the possible strength Δ_J of the uncorrelated Gaussian static disorder in transfer integrals δJ_{mn} is approximately $\Delta_J \approx 0.15\ J_0$. That is why for this type of static disorder we have taken the strengths

$$\Delta_J \in \langle 0.025\ J_0, 0.300\ J_0 \rangle.$$

Other above mentioned types of static disorder also manifest themselves through the fluctuations of transfer integrals and therefore we have taken their strengths in connection with strength ΔJ:

a) uncorrelated fluctuations of radial positions of molecules δr_m

$$\Delta_r \in \langle 0.010\ r_0, 0.30\ r_0 \rangle,$$

b) uncorrelated fluctuations of angular positions of molecules $\delta\nu_m$

$$\Delta_\nu \in \langle 0.001\ \pi, 0.022\ \pi \rangle,$$

c) uncorrelated fluctuations of bacteriochlorophyll dipole moment directions $\delta\vartheta_m$

$$\Delta_\vartheta \in \langle 0.01\ \pi, 0.20\ \pi \rangle.$$

In all cases calculations were done for 10000 realizations of static disorder.

IV. Results and Discussion

Influence of various types of static disorder on Hamiltonian (namely on the nearest neighbour transfer integrals) of B850 ring from LH2 complex is investigated in present paper. Distributions of the nearest neighbour transfer integral $J_{m,m+1}$ were calculated for above mentioned four types of static disorder. These distributions are graphically presented in two ways – mainly by contour plots and also by line plots. Sample expected values $E(J_{m,m+1})$ and values of $E(J_{m,m+1}) \pm \sqrt{D(J_{m,m+1})}$
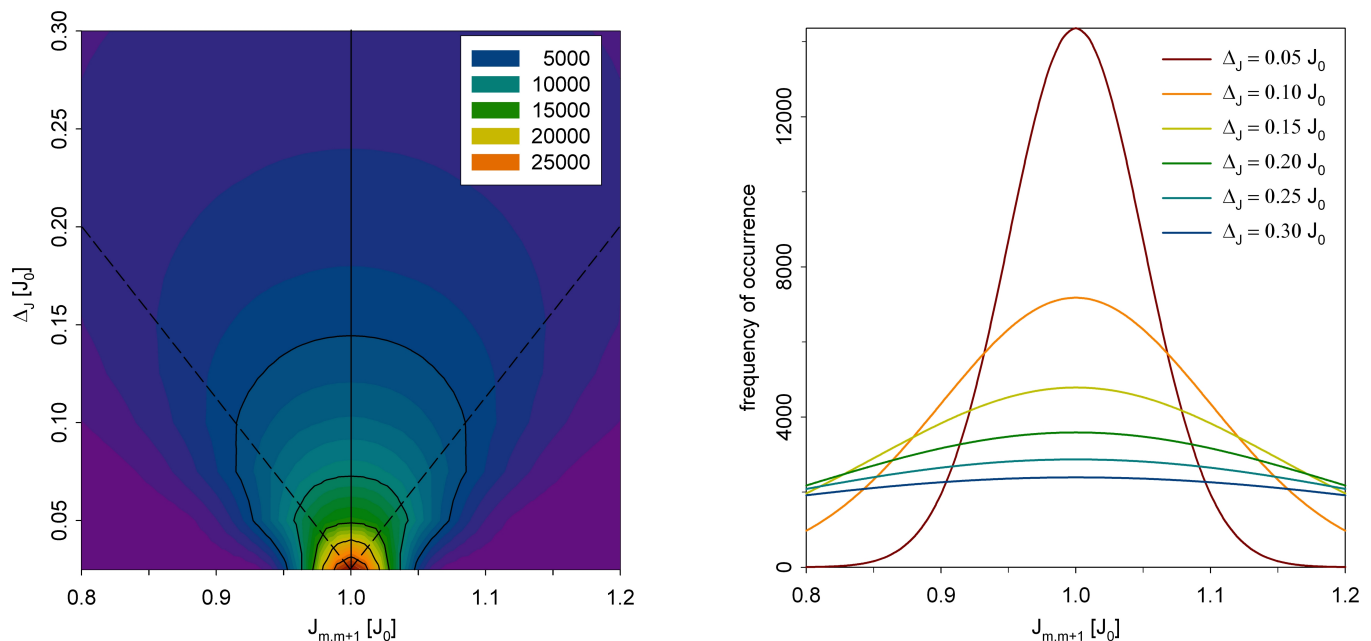

Fig. 5. Distributions of the nearest neighbour transfer integrals $J_{m,m+1}$ for B850 ring from LH2 complex – uncorrelated Gaussian fluctuations of transfer integrals $\delta J_{m,m+1}$ (strengths of static disorder $\Delta_J \in \langle 0.02\ J_0, 0.30\ J_0 \rangle$).
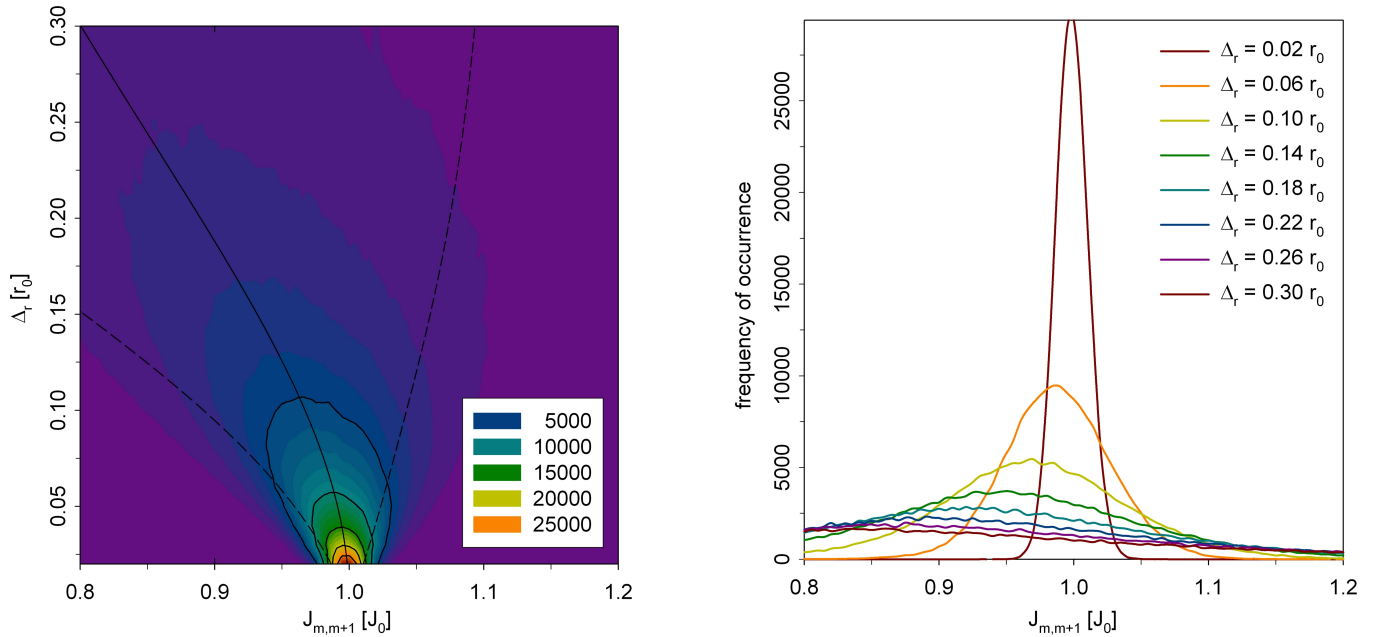
Fig. 6. Distributions of the nearest neighbour transfer integrals $J_{m,m+1}$ for B850 ring from LH2 complex – uncorrelated Gaussian fluctuations in radial positions of molecules on the ring δr_m (strengths of static disorder $\Delta_r \in \langle 0.02\ r_0, 0.30\ r_0 \rangle$).

Δ_r	expected value $E(J_{m,m+1})$	standard deviation $\sqrt{D(J_{m,m+1})}$	skewness α_3	kurtosis α_4	coefficient of variation c
0.02 r_0	0.999 J_0	0.012 J_0	0.083	0.030	0.01204
0.06 r_0	0.988 J_0	0.040 J_0	-0.034	0.506	0.04029
0.10 r_0	0.967 J_0	0.075 J_0	-0.309	1.230	0.07806
0.14 r_0	0.939 J_0	0.118 J_0	-0.447	1.446	0.12515
0.18 r_0	0.907 J_0	0.163 J_0	-0.434	1.277	0.17933
0.22 r_0	0.872 J_0	0.208 J_0	-0.327	1.031	0.23844
0.26 r_0	0.836 J_0	0.252 J_0	-0.165	0.890	0.30097
0.30 r_0	0.800 J_0	0.293 J_0	0.024	0.903	0.36590

TABLE I

EXPECTED VALUE, STANDARD DEVIATION, SKEWNESS, KURTOSIS AND COEFFICIENT OF VARIATION FOR THE NEAREST NEIGHBOUR
TRANSFER INTEGRAL $J_{m,m+1}$ DISTRIBUTIONS FOR UNCORRELATED GAUSSIAN FLUCTUATIONS δr_m (EIGHT STRENGTHS Δ_r)

are also drawn in contour plots. Here $\sqrt{D(J_{m,m+1})}$ is sample standard deviation. Additionally, we calculated sample skewness α_3, sample kurtosis α_4 and sample coefficient of variation c. These statistical characteristics were calculated as follows:

(i) sample expected value

$$E(J_{m,m+1}) = \frac{1}{n} \sum_{i=1}^{n} J_{m,m+1}, \qquad (15)$$

(ii) sample standard deviation

$$\sqrt{D(J_{m,m+1})} = \sqrt{\frac{1}{(n-1)} M_2}, \qquad (16)$$

(iii) sample skewness

$$\alpha_3 = \frac{n^{\frac{5}{2}}}{(n-1)(n-2)} \frac{M_3}{M_2^{\frac{3}{2}}}, \qquad (17)$$

(iv) sample kurtosis

$$\alpha_4 = \frac{n^2}{(n-2)(n-3)} \left[\frac{n(n+1)}{n-1} \frac{M_4}{M_2^2} - 3 \right], \quad (18)$$

(v) sample coefficient of variation

$$c = \sqrt{D(J_{m,m+1})} / E(J_{m,m+1}). \qquad (19)$$

Here

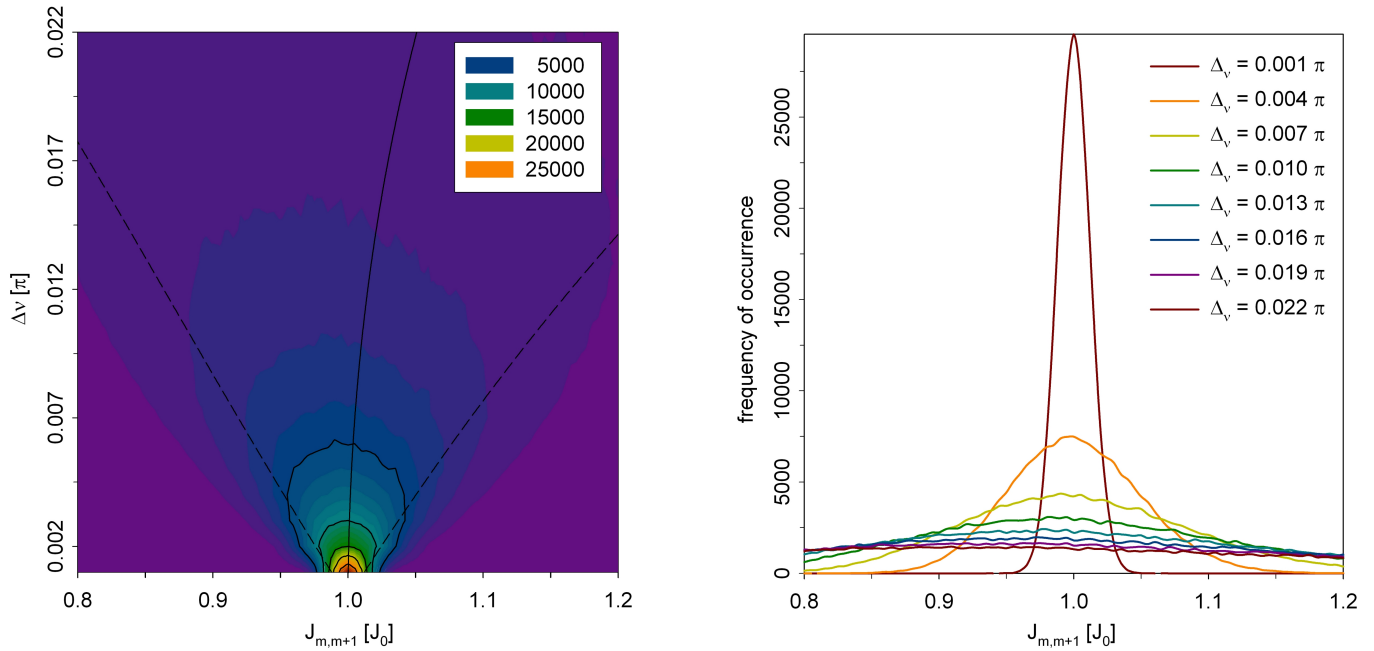$$M_k = \sum_{i=1}^{n} [J_{m,m+1} - E(J_{m,m+1})]^k \qquad (20)$$

Fig. 7. Distributions of the nearest neighbour transfer integrals $J_{m,m+1}$ for B850 ring from LH2 complex – uncorrelated Gaussian fluctuations in angular positions of molecules on the ring $\delta\nu_m$ (strengths of static disorder $\Delta_\nu \in \langle 0.001\ \pi, 0.022\ \pi\rangle$).

Δ_ν	expected value $E(J_{m,m+1})$	standard deviation $\sqrt{D(J_{m,m+1})}$	skewness α_3	kurtosis α_4	coefficient of variation c
$0.001\ \pi$	$1.000\ J_0$	$0.012\ J_0$	0.042	0.004	0.01224
$0.004\ \pi$	$1.002\ J_0$	$0.049\ J_0$	0.189	0.065	0.04872
$0.007\ \pi$	$1.005\ J_0$	$0.086\ J_0$	0.339	0.211	0.08560
$0.010\ \pi$	$1.010\ J_0$	$0.124\ J_0$	0.494	0.455	0.12310
$0.013\ \pi$	$1.017\ J_0$	$0.164\ J_0$	0.657	0.815	0.16153
$0.016\ \pi$	$1.026\ J_0$	$0.206\ J_0$	0.834	1.327	0.20122
$0.019\ \pi$	$1.037\ J_0$	$0.251\ J_0$	1.018	1.959	0.24245
0.022π	$1.050\ J_0$	$0.298\ J_0$	1.164	2.348	0.28426

TABLE II

EXPECTED VALUE, STANDARD DEVIATION, SKEWNESS, KURTOSIS AND COEFFICIENT OF VARIATION FOR THE NEAREST NEIGHBOUR TRANSFER INTEGRAL $J_{m,m+1}$ DISTRIBUTIONS FOR UNCORRELATED GAUSSIAN FLUCTUATIONS $\delta\nu_m$ (EIGHT STRENGTHS Δ_ν)

and n is the number of cases in our samples ($n = 180000$). It corresponds with dimension of Hamiltonian ($N = 18$) and number of static disorder realizations (10000).

Uncorrelated Gaussian distributions of $J_{m,m+1}$ are presented in Figure 5 for comparison to other types of static disorder that are connected with deviations of ring geometry. For this type of fluctuations ($\delta J_{m,m+1}$), of course, the expected value of the distribution of the nearest neighbour transfer integrals $J_{m,m+1}$ is independent of the strength of static disorder, i.e. $E(J_{m,m+1}) = J_0$, and the strength of static disorder Δ_J equals the standard deviation $\sqrt{D(J_{m,m+1})}$.

Figure 6 shows the distributions of $J_{m,m+1}$ for Gaussian uncorrelated static disorder δr_m in radial positions

of molecules on the ring. The distributions of $J_{m,m+1}$ for other two above mentioned types of static disorder can be seen in Figure 7 (Gaussian uncorrelated fluctuations of angular positions of molecules on the ring $\delta\nu_m$) and in Figure 8 (Gaussian uncorrelated fluctuations of molecular dipole moment directions $\delta\vartheta_m$). For these three types of static disorder (connected with deviations in ring geometry) expected value $E(J_{m,m+1})$ depends on static disorder strength. Dependencies of $E(J_{m,m+1})$ and $\sqrt{D(J_{m,m+1})}$ on corresponding static disorder strength are presented in Figure 6 – left column (δr_m), Figure 7 – left column ($\delta\nu_m$) and Figure 8 – left column ($\delta\vartheta_m$). Values of $E(J_{m,m+1})$, $\sqrt{D(J_{m,m+1})}$, α_3, α_4 and c (see Eq. (15) – Eq. (19)) for chosen static disorder strengths
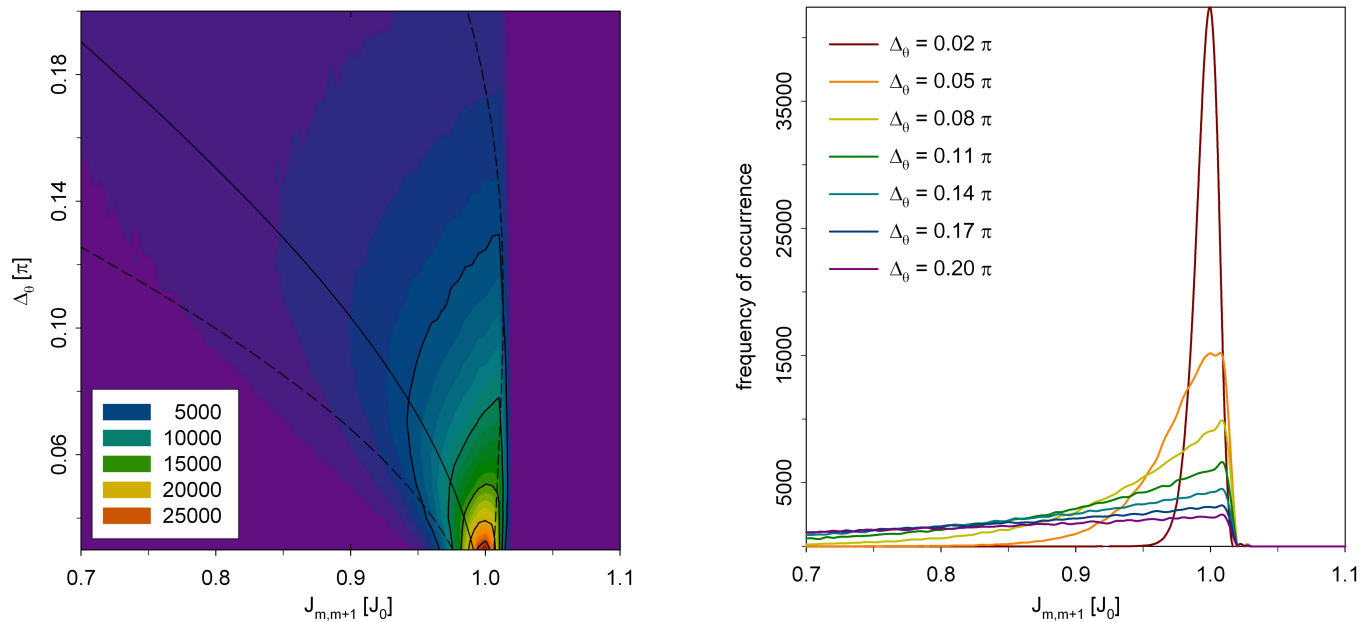
Fig. 8. Distributions of the nearest neighbour transfer integrals $J_{m,m+1}$ for B850 ring from LH2 complex – uncorrelated Gaussian fluctuations in directions of molecular dipole moments $\delta\vartheta_m$ (strengths of static disorder $\Delta_\vartheta \in \langle 0.02\,\pi, 0.20\,\pi \rangle$).

Δ_ϑ	expected value $E(J_{m,m+1})$	standard deviation $\sqrt{D(J_{m,m+1})}$	skewness α_3	kurtosis α_4	coefficient of variation c
$0.02\,\pi$	$0.996\,J_0$	$0.009\,J_0$	-0.760	0.951	0.00902
$0.05\,\pi$	$0.976\,J_0$	$0.033\,J_0$	-1.676	4.585	0.03390
$0.08\,\pi$	$0.939\,J_0$	$0.073\,J_0$	-1.952	5.819	0.07766
$0.11\,\pi$	$0.888\,J_0$	$0.126\,J_0$	-1.941	5.350	0.14144
$0.14\,\pi$	$0.824\,J_0$	$0.186\,J_0$	-1.811	4.260	0.22591
$0.17\,\pi$	$0.752\,J_0$	$0.250\,J_0$	-1.629	3.056	0.33232
$0.20\,\pi$	$0.674\,J_0$	$0.312\,J_0$	-1.428	1.964	0.46295

TABLE III

EXPECTED VALUE, STANDARD DEVIATION, SKEWNESS, KURTOSIS AND COEFFICIENT OF VARIATION FOR THE NEAREST NEIGHBOUR
TRANSFER INTEGRAL $J_{m,m+1}$ DISTRIBUTIONS FOR UNCORRELATED GAUSSIAN FLUCTUATIONS $\delta\vartheta_m$ (SEVEN STRENGTHS Δ_ϑ)

are presented in Table I (δr_m), Table II ($\delta\nu_m$) and Table III ($\delta\vartheta_m$).

In case of Gaussian distribution of transfer integrals $J_{m,m+1}$ expected value $E(J_{m,m+1})$ is independent of static disorder strength ($E(J_{m,m+1}) = J_0$) and standard deviation $\sqrt{D(J_{m,m+1})}$ equals the strength of static disorder $\sqrt{D(J_{m,m+1})} = \Delta_J$. That is why, coefficient of variation c corresponds to strength of static disorder Δ_J, i.e. $c = \Delta_J/J_0$ (see Eq. (19)). In this case skewness α_3 and kurtosis α_4 equal zero, i.e. they are also independent of static disorder strength Δ_J.

If we consider other types of static disorder (connected with deviations in ring geometry – δr_m, $\delta\nu_m$, $\delta\vartheta_m$), Gaussian distribution of molecular positions or dipole moment directions results in non–Gaussian dis-

tribution of transfer integrals $J_{m,m+1}$. That is why, expected value $E(J_{m,m+1})$, skewness α_3 and kurtosis α_4 are nonconstant and standard deviation $\sqrt{D(J_{m,m+1})}$ does not equal the strength of static disorder (see Figures $6 - 8$ and Tables I – III). As concerns expected value $E(J_{m,m+1})$, we can see decrease of it for increasing static disorder strength in case of fluctuations in radial positions of molecules on the ring δr_m (see Figure 6 and Table I) and fluctuations in molecular dipole moment directions $\delta\vartheta_m$ (see Figure 8 and Table III). On the other hand, $E(J_{m,m+1})$ increases with growing strength of static disorder in angular positions of molecules on the ring $\delta\nu_m$ (see Figure 7 and Table II). In all these three cases dependence of standard deviation $\sqrt{D(J_{m,m+1})}$ on static disorder strength is nonlinear. The most important

change of expected value occurs in case of fluctuations of molecular dipole moment directions $\delta\vartheta_m$. In contrast with this type of static disorder the changes of $E(J_{m,m+1})$ are very low for fluctuations in angular positions of molecules $\delta\nu_m$. Non–Gaussian distributions of $J_{m,m+1}$ manifest themselves by nonzero skewness and kurtosis in all three cases of static disorder connected with deviations in ring geometry. Skewness is negative for static disorder in radial positions of molecules δr_m and static disorder in directions of molecular dipole moments $\delta\vartheta_m$. Contrary, in case of static disorder in angular positions of molecules $\delta\nu_m$ the distribution of $J_{m,m+1}$ is skewed to right hand side. Most significant skewness can be seen in case of static disorder in directions of molecular dipole moments $\delta\vartheta_m$ (Figure 8). All these three distributions have higher kurtosis in comparison with Gaussian distribution of $J_{m,m+1}$.

Due to nonconstant expected value, influences of different types of fluctuations to distribution of $J_{m,m+1}$ can be compared using coefficient of variation. Our previous investigations [35] led to suitable strength of static disorder in transfer integrals $\Delta_J \approx 0.15\ J_0$ and consequently $c \approx 0.15$. As concerns other types od static disorder, approximately same value of coefficient of variation corresponds to the following disorder strengths: $\Delta_r \approx 0.16\ r_0$, $\Delta_\nu \approx 0.012\pi$ and $\Delta_\vartheta \approx 0.11\pi$.

V. Conclusions

Comparison of the results obtained within different types of static disorder can be summarized as follows. Expected value of the nearest neighbour transfer integral distribution depends on static disorder strength for all presented types of fluctuations connected with ring geometry. The most essential change appears in case of static disorder in dipole moment directions. In this case also the dependence of standard deviation of the distribution on the static disorder strength has the highest nonlinearity. This is connected with the highest skewness of this distribution. Through the comparison of coefficient of variation we are able to estimate suitable strength of static disorder types connected with ring geometry fluctuations.

References

[1] D. W. Lawlor, *Photosynthesis*, Spriger, New York 2001.
[2] R. van Grondelle and V. I. Novoderezhkin, Energy transfer in photosynthesis: experimental insights and quantitative models, *Phys. Chem. Chem. Phys.* 8, 2003, pp. 793–807.
[3] G. McDermott, et al., Crystal structure of an integral membrane light-harvesting complex from photosynthetic bacteria, *Nature* 374, 1995, pp. 517–521.
[4] M. Z. Papiz, et al., The structure and thermal motion of the B 800-B850 LH2 complex from Rps. acidophila at 2.0 A resolution and 100 K: new structural features and functionally relevant motions, *J. Mol. Biol.* 326, 2003, pp. 1523–1538.
[5] W. P. F. de Ruijter, et al., Observation of the Energy–Level Structure of the Low–Light Adapted B800 LH4 Complex by Single–Molecule Spectroscopy, *Biophys. J.* 87, 2004, pp. 3413–3420.

[6] R. Kumble and R. Hochstrasser, Disorder–induced exciton scattering in the light–harvesting systems of purple bacteria: Influence on the anisotropy of emission and band $\rightarrow$ band transitions, *J. Chem. Phys.* 109, 1998, pp. 855–865.
[7] V. Nagarajan, et al., Femtosecond pump–probe spectroscopy of the B850 antenna complex of Rhodobacter sphaeroides at room temperature, *J. Phys. Chem. B* 103, 1999, pp. 2297–2309.
[8] V. Nagarajan and W. W. Parson, Femtosecond fluorescence depletion anisotropy: Application to the B850 antenna complex of Rhodobacter sphaeroides, *J. Phys. Chem. B* 104, 2000, pp. 4010–4013.
[9] V. Čápek, I. Barvík and P. Heřman, Towards proper parametrization in the exciton transfer and relaxation problem: dimer, *Chem. Phys.* 270, 2001, pp. 141–156.
[10] P. Heřman and I. Barvík, Towards proper parametrization in the exciton transfer and relaxation problem. II. Trimer, *Chem. Phys.* 274, 2001, pp. 199–217.
[11] P. Heřman, I. Barvík and M. Urbanec, Energy relaxation and transfer in excitonic trimer, *J. Lumin.* 108, 2004, pp. 85–89.
[12] P. Heřman, et al., Exciton scattering in light–harvesting systems of purple bacteria, *J. Lumin.* 94–95, 2001, pp. 447–450.
[13] P. Heřman and I. Barvík, Non–Markovian effects in the anisotropy of emission in the ring antenna subunits of purple bacteria photosynthetic systems, *Czech. J. Phys.* 53, 2003, pp. 579–605.
[14] P. Heřman, et al., Influence of static and dynamic disorder on the anisotropy of emission in the ring antenna subunits of purple bacteria photosynthetic systems, *Chem. Phys.* 275, 2002, pp. 1–13.
[15] P. Heřman and I. Barvík, Temperature dependence of the anisotropy of fluorescence in ring molecular systems, *J. Lumin.* 122–123, 2007, pp. 558–561.
[16] P. Heřman, D. Zapletal and I. Barvík, Computer simulation of the anisotropy of fluorescence in ring molecular systems: Influence of disorder and ellipticity, *Proc. IEEE 12th Int. Conf. on Computational Science and Engineering*, Vancouver: IEEE Comp. Soc., 2009, pp. 437–442.
[17] P. Heřman and I. Barvík, Coherence effects in ring molecular systems, *Phys. Stat. Sol. C* 3, 2006, 3408–3413.
[18] P. Heřman, D. Zapletal and I. Barvík, The anisotropy of fluorescence in ring units III: Tangential versus radial dipole arrangement, *J. Lumin.* 128, 2008, pp. 768–770.
[19] P. Heřman, I. Barvík and D. Zapletal, Computer simulation of the anisotropy of fluorescence in ring molecular systems: Tangential vs. radial dipole arrangement, *Lecture Notes in Computer Science* 5101, 2008, pp. 661–670.
[20] P. Heřman, D. Zapletal and I. Barvík, Lost of coherence due to disorder in molecular rings, *Phys. Stat. Sol. C* 6, 2009, pp. 89–92.
[21] P. Heřman, D. Zapletal and J. Šlégr, Comparison of emission spectra of single LH2 complex for different types of disorder, *Phys. Proc.* 13, 2011, pp. 14–17.
[22] D. Zapletal and P. Heřman, Simulation of molecular ring emission spectra: localization of exciton states and dynamics, *Int. J. Math. Comp. Sim.* 6, 2012, pp. 144–152.
[23] M. Horák, P. Heřman and D. Zapletal, Simulation of molecular ring emission spectra – LH4 complex: localization of exciton states and dynamics, *Int. J. Math. Comp. Sim.* 7, 2013, pp. 85–93.
[24] P. Heřman and D. Zapletal, Intermolecular coupling fluctuation effect on absorption and emission spectra for LH4 ring, *Int. J. Math. Comp. Sim.* 7, 2013, pp. 249–257.
[25] M. Horák, P. Heřman and D. Zapletal, Modeling of emission spectra for molecular rings – LH2, LH4 complexes, *Phys. Proc.* 44, 2013, pp. 10–18.
[26] P. Heřman, D. Zapletal and M. Horák, Emission spectra of LH2 complex: full Hamiltonian model, *Eur. Phys. J. B* 86, 2013, art. no. 215.
[27] P. Heřman and D. Zapletal, Emission Spectra of LH4 Complex: Full Hamiltonian Model, *Int. J. Math. Comp. Sim.* 7, 2013, pp. 448–455.
[28] P. Heřman and D. Zapletal, Simulation of Emission Spectra for LH4 Ring: Intermolecular Coupling Fluctuation Effect, *Int. J. Math. Comp. Sim.* 8, 2014, pp. 73–81.
[29] D. Zapletal and P. Heřman, Photosynthetic complex LH2 – Absorption and steady state fluorescence spectra, *Energy* 77, 2014, pp. 212–219.
[30] P. Heřman and D. Zapletal, Simulations of emission spectra for LH4 Ring – Fluctuations in radial positions of molecules, *Int. J. Biol. Biomed. Eng.* 9, 2015, pp. 65–74.
[31] P. Heřman and D. Zapletal, Computer simulation of emission and absorption spectra for LH2 ring, *LNEE* 343, 2015, pp. 221–234.

[32] P. Heřman and D. Zapletal, Modeling of Absorption and Steady State Fluorescence Spectra of Full LH2 Complex (B850 – B800 Ring), *Int. J. Math. Mod. Meth. Appl. Sci.* 9, 2015, pp. 614–623.

[33] P. Heřman and D. Zapletal, Modeling of Emission and Absorption Spectra of LH2 Complex (B850 and B800 Ring) – Full Hamiltonian Model, *Int. J. Math. Comp. Sim.* 10, 2016, pp. 208–217.

[34] P. Heřman and D. Zapletal, B–α/B–β Ring from Photosynthetic Complex LH4, Modeling of Absorption and Fluorescence Spectra, *Int. J. Math. Comp. Sim.* 10, 2016, pp. 332–344.

[35] P. Heřman, I. Barvík and D. Zapletal, Energetic disorder and exciton states of individual molecular rings, *J. Lumin.* 119–120, 2006, pp. 496–503.

[36] C. Hofmann, T. J. Aartsma and J. Kőhler, Energetic disorder and the B850–exciton states of individual light–harvesting 2 complexes from Rhodopseudomonas acidophila, *Chem. Phys. Lett.* 395, 2004, pp. 373–378.